Phys. Med. Biol. **46** (2001) 975–982 www.iop.org/Journals/pb PII: S0031-9155(01)18589-1

Beat-to-beat analysis method for magnetocardiographic recordings during interventions

P Takala[1,2], H Hänninen[2,3], J Montonen[1,2], M Mäkijärvi[2,3], J Nenonen[1,2], L Toivonen[2,3] and T Katila[1,2]

[1] Laboratory of Biomedical Engineering, Helsinki University of Technology, FIN-02015 HUT, Finland
[2] BioMag Laboratory, Medical Engineering Centre, Helsinki University Central Hospital, FIN-00029 HUCH, Finland
[3] Division of Cardiology, Helsinki University Central Hospital, FIN-00029 HUCH, Finland

E-mail: panu.takala@hut.fi

Received 2 November 2000, in final form 5 January 2001

Abstract

Multichannel magnetocardiography (MCG) during exercise testing has been shown to detect myocardial ischaemia in patients with coronary artery disease. Previous studies on exercise MCG have focused on one or few time intervals during the recovery period and only a fragment of the data available has been utilized.

We present a method for beat-to-beat analysis and parametrization of the MCG signal. The method can be used for studying and quantifying the changes induced in the MCG by interventions. We test the method with data recorded in bicycle exercise testing in healthy volunteers and patients with coronary artery disease. Information in all cardiac cycles recorded during the recovery period of exercise MCG testing is, for the first time, utilized in the signal analysis.

Exercise-induced myocardial ischaemia was detected by heart rate adjustment of change in magnetic field map orientation. In addition to the ST segment, the T wave in the MCG was also found to provide information related to myocardial ischaemia. The method of analysis efficiently utilizes the spatial and temporal properties of multichannel MCG mapping, providing a new tool for detecting and quantifying fast phenomena during interventional MCG studies. The method can also be applied to an on-line analysis of MCG data.

1. Introduction

Multichannel magnetocardiography (MCG) allows an extensive spatial and temporal sampling of the magnetic field evoked by bioelectric currents in the heart (Oeff 1993). In dynamic studies in particular, such as exercise testing, feature extraction and efficient utilization of the multichannel data are important points when clinical applications of MCG are developed. Electrocardiography (ECG) during exercise is the most widely used screening method for coronary artery disease (CAD). Its sensitivity to CAD, however, is limited (Gianrossi *et al* 1989).

Improved possibilities for the treatment of CAD have increased the need for fast and non-invasive methods to detect the ischaemic myocardium and to assess its extent and location. The MCG is a novel, fast and non-contact mapping technique. In addition to temporal parameters resembling those used in 12-lead ECG analysis, the spatial features of the magnetic field over the thorax can be quantified and utilized in detection of ischaemia. Ischaemia has been shown to cause a rotation of the magnetic field distribution recorded in exercise testing (Hänninen *et al* 2000).

The number of exercise MCG studies published is, however, small. The main reason for this is the absence of commercially available ergometers suitable for such studies. The effect of stress in the MCG of healthy subjects has been studied (Brockmeier *et al* 1994, 1997, Takala *et al* 1999). In addition, changes induced by ischaemic injury current in the MCG signal have been quantified by calculation of rotation in the magnetic field maps (MFM) (Hänninen *et al* 2000, Van Leeuwen *et al* 1999) as well as by measurement of QT time dispersion (Hailer *et al* 1999). MCG has also showed potential for the localization of transient and chronic ischaemia (Pesola *et al* 1999).

Previous studies on signal-averaged exercise MCG data have focused on analysis at one or a few intervals of the recovery period. Thereby, most of the data recorded have been excluded from the signal analysis. In the ECG, the development of the ST-segment depression during exercise and recovery is an important factor in evaluation of ischaemia. So far, no studies on the development of ischaemia-induced changes in the MCG data recorded during exercise testing have been reported. Heart rate adjustment of ST depression has been shown to improve the performance of exercise ECG in the detection of ischaemia (Kligfield *et al* 1989). In this paper, we present a method for beat-to-beat analysis of the MCG mapping and apply it to data recorded during the recovery phase of bicycle exercise testing in healthy controls and CAD patients. We utilize the heart rate adjusted alteration in the magnetic field distribution to quantify ischaemia-induced change in the MCG.

2. Methods

2.1. Subjects

We recorded magnetocardiograms during supine exercise testing in two healthy volunteers and in three patients with CAD. Each patient had a significant ($>50\%$ luminal diameter) stenosis in different main coronary branches: left anterior descending (LAD), left circumflex (LCX), and right coronary artery (RCA). All patients had anginal pain and ECG-documented ischaemia with a $\geqslant 0.1$ mV ST-segment depression in standard upright bicycle exercise testing. None of the patients had suffered myocardial infarction or showed abnormal Q-waves in the 12-lead ECG. All subjects had normal wall motion and wall thickness in echocardiography.

2.2. Exercise measurement

The subjects underwent supine exercise MCG recordings in a magnetically shielded room (Paavola *et al* 2000). The MCG signals were recorded over the chest with a 67-channel cardiomagnetometer covering a circular area with a diameter of 30 cm over the chest (Montonen *et al* 2000). The centre of the sensor array was placed 15 cm down from the

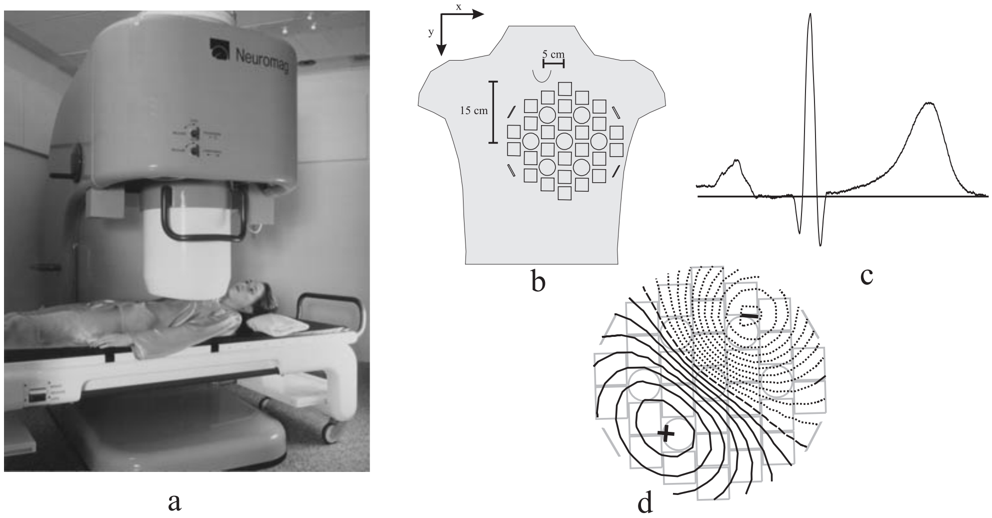

Figure 1. (*a*) The 67-channel cardiomagnetometer. (*b*) The positioning of the sensor array over the chest. Locations of planar gradiometer units recording $\partial B_z/\partial x$ and $\partial B_z/\partial y$ are marked with squares and coaxial gradiometers recording $\partial B_z/\partial z$ are indicated by circles. Here, z is normal to the surface of the sensor. (*c*) An example of the MCG signal on one channel. (*d*) Distribution of the magnetic field component B_z over the mapped area at one time instant. Positive values indicate magnetic flux towards the chest. Zero field is marked with a broken curve.

jugular notch and 5 cm to the left of the midsternal line (figure 1). Data were recorded with a sampling frequency of 1 kHz and band-pass filtered to 0.03–300 Hz. Twelve-lead ECG was recorded simultaneously with the MCG.

Exercise testing was performed with a non-magnetic ergometer designed for cardiomagnetic measurements. A baseline recording of 5 min at rest preceded a graded exercise test with 2 min load intervals. The cessation criteria were as recommended by the American Heart Association (Fletcher *et al* 1995), and the recording was sustained up to 10 min after exercise.

2.3. Data analysis

2.3.1. QRS complex detection. An ECG channel with a high signal amplitude was selected for automatic detection of the QRS complexes in the data recorded during the recovery period of the exercise test. The trigger time was detected as the time instant of the steepest signal slope in one template beat. The trigger time search was then carried out for the whole recording. By calculating the highest signal correlation with the template, the corresponding time instants in signal morphology were found in all QRS complexes. The trigger times were finally used to determine other time points of each cardiac cycle (figure 2). Here, an assumption was made that the duration of the QRS complex does not change significantly during the measurement. To take into account the change in signal morphology with changing heart rate, the ST segment was defined as the second quarter of the time interval from the QRS complex offset to the T-wave apex.

2.3.2. Baseline estimation. Time offsets from the trigger time to the beginning of a 20 ms baseline interval, as well as to the onset and offset of the QRS complex, were visually defined in

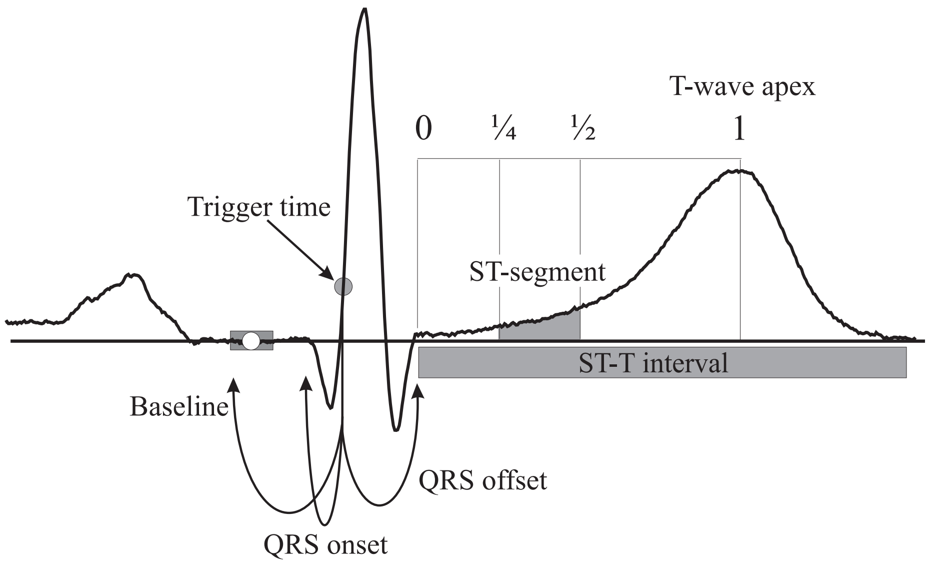

Figure 2. Time selection within one cardiac cycle. The QRS complex onset and offset as well as the baseline interval were defined with respect to the trigger time within the QRS complex. The signal baseline node was the signal mean over a baseline interval of 20 ms. The ST–T interval begins at the QRS complex offset and ends at the T-wave offset. The T-wave apex was defined as the highest absolute value of signal within the ST–T interval. The ST segment was defined as the second quarter of the time interval from the QRS complex offset to the T-wave apex.

one cardiac cycle and applied to all complexes (figure 2). For each cardiac cycle, a baseline was determined as explained in figure 2. A cubic spline baseline estimate through the baseline points at the PQ intervals was calculated for each channel, and subtracted from the corresponding signal (Meyer and Keiser 1977).

2.3.3. Extraction of a magnetic field map. To extract a magnetic field map (MFM) of the T-wave apex from one cardiac cycle, the ST–T interval was first defined. Here, a crude estimate for the T-wave offset was obtained as QRS onset + 450 ms $\times$ (RR interval)$^{1/3}$ (Fridericia 1920). The T-wave apex time on each channel was derived as the highest signal deviation from the baseline within the ST–T interval. To obtain one T-apex time for each cardiac cycle, the median T-apex time over all channels was calculated. T-apex times of all cardiac cycles in the recovery data were found, and on each channel the mean values of signal over the T apex ± 10 ms were extracted for further analysis.

The ST segment was defined as the second quarter from the QRS offset to the T apex (figure 2). The mean signal value over the ST segment was calculated on all channels to obtain the ST-segment level in the ECG and to form an ST-segment integral map in the MCG. ST-segment values in all cardiac cycles during recovery were extracted for further analysis. To increase the signal to noise ratio, the sequence of MFMs was mean filtered with a window length of 11 MFMs.

2.3.4. Magnetic field map parametrization. The surface gradient method, introduced earlier by Hänninen *et al* (2000), was used to calculate the orientations of the MFMs. Briefly, the location and the direction of the largest spatial gradient ($\partial B_z/\partial x$, $\partial B_z/\partial y$) of the signal distribution in the measurement plane was first computed. The angle between the direction

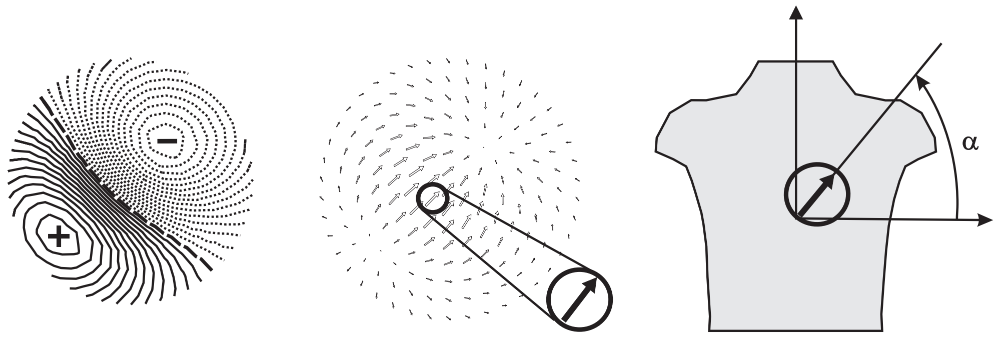

a b c

Figure 3. Parametrization of magnetic field maps (MFM). (*a*) An example of an MFM. (*b*) Surface gradients of the data in (*a*). The largest gradient and its orientation are indicated with a large arrow. (*c*) The MFM angle α was measured with respect to the subject's right–left line.

of the largest gradient and the patient's right–left line was then defined as the MFM angle (figure 3).

2.3.5. Quantification of change in magnetic field maps. Both the ST-segment MFM angles during the recovery period, and the T-wave MFM angles from 1 to 10 min after exercise were used for the quantification of changes in the MFMs. The analysis was performed separately for each subject for the ST segment and the T wave. To reject artefacts, the mean and standard deviation (SD) of the MFM angle was first calculated and values deviating from the mean more than 2 SD were discarded from further analysis. Thereafter, each MFM angle was plotted against the instantaneous heart rate, determined from the duration of the RR interval at the time of MFM extraction. A regression line was fitted to these data. The absolute value of the line slope was calculated both in the ST segment (MFM ST/HR slope) and T-wave (MFM T/HR slope) data and used as a parameter to quantify changes in the MFMs.

2.3.6. Quantification of change in ST-segment level in the ECG. The ST-segment data on each ECG lead were plotted as a function of heart rate, and values outside mean ± 2 SD were discarded. A line was fitted in the data, and the steepest negative line slope within all leads (ECG ST/HR slope) was calculated.

3. Results

By viewing the baseline-corrected MCG signal, calculation of the baseline estimate was found to efficiently cancel the low-frequency magnetic noise in the data. At the beginning of the recovery, where the noise due to heavy breathing was more extensive than at rest, a higher heart rate enabled more frequent sampling of the PQ intervals and improved the noise reduction.

The time instants of QRS complex onset and offset, determined in the template beat in respect of the trigger point, matched well with the QRS complex in other cardiac cycles. In multichannel recordings, the T-wave apexes on different channels do not coincide. The T-wave apex times used for the MFM extraction coincided with the T-wave apexes at the channels with high T-wave amplitude. By calculation of the mean of T-wave apex times, problems due to biphasic T-waves were also avoided.

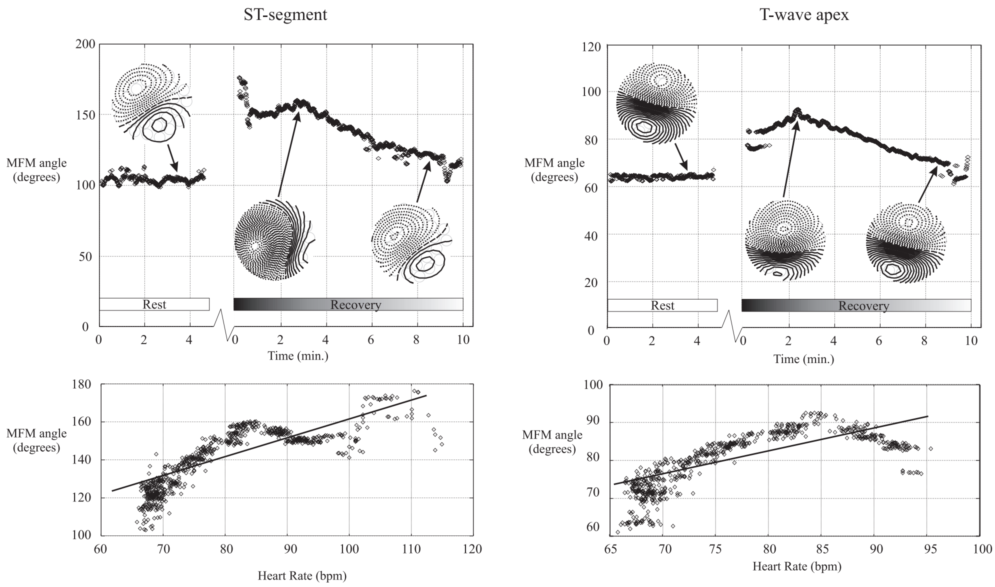

Figure 4. Magnetic field map angle data and examples of field distributions in the LCX patient. Left, the ST-segment data; right, the T-wave apex data. In the upper panels, the MFM angles at rest and during the recovery from exercise are plotted against time. The exercise data have been omitted. At rest the MFM angle has an approximately constant value. Immediately after exercise the angle is tilted, and during the recovery it returns close to the value at rest. Arrows indicate the time instants and angle values for the MFMs shown. In the lower panels, the MFM angle is plotted against the heart rate. All the recovery data for the ST segment, and data from 1 to 10 min after exercise for the T wave are shown. Straight lines through the data sets indicate the regression lines used for rough quantification of the change in the MFM angles. The line slope for the ST segment is 1.0 deg bpm^{-1} and for the T wave 0.6 deg bpm^{-1}.

Table 1. Linear regression coefficients for the rotation of the magnetic field map (MFM) at the ST segment and at the T wave, and for the ST-segment level change in the ECG in all subjects. HR = heart rate, bpm = beats per minute.

Subject	MFM ST/HR slope (deg bpm^{-1})	MFM T/HR slope (deg bpm^{-1})	ECG ST/HR slope (μV bpm^{-1})
Control 1	0.34	0.15	−1.45
Control 2	0.17	0.05	−0.97
LAD	1.77	0.16	−1.70
LCX	1.04	0.60	−2.64
RCA	0.82	0.99	−1.30

In our control subjects, exercise induced only a small rotation in the MFMs and the slopes of the regression lines were mild. The heart rate adjusted changes in MFM angles and ST-segment level in the ECG are shown in table 1 for all subjects. The MFM angles changed in CAD patients more than in controls, and the regression line slopes were steeper. Only in the LAD patient was the T-wave MFM slope of the same order as in one of the controls. In two CAD patients, the ST/HR slope in the 12-lead ECG was steeper than in the controls, but in the RCA patient the slope was less steep than in one control subject.

Figure 4 shows an example of the development of the ST-segment and T-wave MFM angle in one CAD patient at rest and during recovery after exercise. At rest, the angle stays approximately at a constant level, whereas after exercise it returns towards the value at rest. The lower panels in figure 4 illustrate the MFM angle as a function of heart rate and the regression lines through the data.

4. Discussion

In this study we present a method for continuous analysis of magnetic field maps recorded in multichannel magnetocardiography. We test the method with data recorded during exercise testing. To our knowledge, all the recovery data recorded in exercise magnetocardiography are analysed here for the first time. We also present the first results of detection of exercise-induced ischaemia by heart rate adjustment of change in magnetic field maps.

Ischaemic injury current in the heart, directed from the lower left toward the upper right chest, results in a well known ST-segment depression in the precordial ECG leads. In the MCG, such a current, in theory, induces a magnetic flux toward the chest at the upper left thorax and outward from the thorax at the central thoracic area. When superposed on the normal MCG signal distribution, this ischaemic field pattern might give rise to a rotation in the MFM pattern. The results obtained in this study support this hypothesis. Rotation of the magnetic field distribution due to ischaemia has also been reported in other studies with signal averaged data (Hänninen *et al* 2000, Van Leeuwen *et al* 1999). The beat-to-beat analysis method presented here allows continuous evaluation of the change in MFM pattern with decaying injury current as a function of time or the heart rate.

The heart rate and thus the signal morphology change during the recovery in exercise testing. In signal averaging, if the complexes are aligned in accordance with the QRS complex, the alteration in the ST–T morphology results in blurring of the signal. Therefore we find the beat-to-beat analysis method presented here more suitable for exercise MCG recordings than signal averaging. To decrease noise and distortions caused, for example, by breathing, we mean filtered the MFM sequence. When applied to data recorded during different interventions, the window length in filtering should be adjusted according to the rate of change of the phenomenon studied.

To quantify the change in the MFM orientation we extracted the data of interest in each beat and used linear regression to detect a trend in the MFM angle. Thereby, information in each cardiac cycle was included in the analysis. The change in MFM orientation was adjusted to heart rate, which has been shown to improve the detection of ischaemia in exercise ECG (Kligfield *et al* 1989). In figure 4, it can be seen that the relation between the MFM angle and the heart rate is not linear during the recovery of exercise testing in the patient with a stenosis in the LCX coronary artery. Also in the ECG, the ST-segment depression in this case had a local maximum at the heart rate of approximately 85 bpm. In the two other patients studied, and especially in the healthy controls, the dependence between MFM angle and heart rate was more linear. The slope of the regression line is only a rough means to quantify the change in MFM angle with heart rate. On the other hand, the injury current decays in each individual patient in a different manner during the recovery, and a more complex model may not be applicable to all subjects.

After extracting MFMs at the segments of interest in each cardiac cycle, parameters other than the orientation of the steepest spatial gradient could also be calculated. Mean filtering of the MFM sequence improves the signal to noise ratio to such an extent that inverse calculation with complex source models could also be applied to detect the injury current (Pesola *et al* 1999). The surface gradient method tested in this work is simple to implement. In some cardiomagnetometers, planar gradiometers measure directly the spatial derivative of the magnetic field (Montonen *et al* 2000). This makes the determination of the MFM orientation an easy and fast task. In all multichannel systems, the gradients can be calculated (Hänninen *et al* 2000). The method presented here is not computationally demanding and it could also be applied to an on-line analysis of MCG measurements.

Only five subjects were studied to test the analysis method developed. No conclusions can thus be made of the performance of the method in detection of ischaemia. However, in all CAD patients the heart rate adjusted change in the MFM orientation was higher than in the controls, both at the ST segment and at the T-wave apex. Studies with larger patient populations are needed to evaluate the performance of the method in ischaemia detection. In this paper, we present a method for extracting data of interest from cardiac recordings. The method was tested here with exercise MCG data and applied to ischaemia detection. Further research is needed to assess its value in other recordings and applications. In addition to MCG, it could be applied to data extraction in body surface potential mapping recordings, for example.

References

Brockmeier K, Comani S, Erne S N, Di Luzio A, Pasquarelli A and Romani G L 1994 Magnetocardiography and exercise testing *J. Electrocardiol.* **27** 137–42

Brockmeier K, Schmitz L, Chavez J, Burghoff M, Koch H, Zimmerman R and Trahms L 1997 Magnetocardiography and 32-lead potential mapping: repolarization in normal subjects during pharmacologically induced stress *J. Cardiovasc. Electrophysiol.* **8** 615–26

Fletcher G F, Balady G, Froelicher V F, Hartley L H, Haskell W L and Pollock M L 1995 Exercise standards. A statement for healthcare professionals from the American Heart Association *Circulation* **91** 580–615

Fridericia L 1920 Systolendauer im Electrocardiogramm bei normalen Menschen und bei Herzkranken *Acta Med. Scand.* **53** 469–86

Gianrossi R, Detrano R, Mulvihill D, Lehman K, Dubach P, Colombo A, McArthur D and Froelicher V 1989 Exercise-induced ST depression in the diagnosis of coronary artery disease: a meta-analysis *Circulation* **80** 87–98

Hailer B, Van Leeuwen P, Lange S and Wehr M 1999 Spatial distribution of QT dispersion measured by magnetocardiography under stress in coronary artery disease *J. Electrocardiol.* **32** 207–16

Hänninen H, Takala P, Mäkijärvi M, Montonen J, Korhonen P, Oikarinen L, Nenonen J, Katila T and Toivonen L 2000 Detection of exercise-induced myocardial ischemia by multichannel magnetocardiography in single vessel coronary artery disease *Ann. Noninv. Electrocardiol.* **5** 147–57

Kligfield P, Ameisen O and Okin P 1989 Heart rate adjustment of ST segment depression for improved detection of coronary artery disease *Circulation* **79** 245–55

Meyer C and Keiser H 1977 Electrocardiogram baseline noise estimation and removal using cubic splines and state-space computation techniques *Comput. Biomed. Res.* **10** 459–70

Montonen J, Ahonen A, Hämäläinen M, Ilmoniemi R J, Laine P, Nenonen J, Paavola M, Simelius K, Simola J and Katila T 2000 Magnetocardiographic functional imaging studies in the BioMag laboratory *Biomag 96, Proc. 10th Int. Conf. on Biomagnetism* (New York: Springer) pp 494–7

Oeff M 1993 Magnetocardiographic mapping *Cardiac Mapping* ed M Shenasa, M Borggrefe *et al* (New York: Futura) pp 383–8

Paavola M, Ilmoniemi R, Sohlström L, Meinander T, Penttinen A and Katila T 2000 High performance magnetically shielded room for clinical measurements *Biomag 96, Proc. 10th Int. Conf. on Biomagnetism* (New York: Springer) pp 87–90

Pesola K, Hänninen H, Lauerma K, Lötjönen J, Mäkijärvi M, Nenonen J, Takala P, Voipio-Pulkki L-M, Toivonen L and Katila T 1999 Current density estimation on the left ventricular epicardium: a potential method for ischemia localization *Biomed. Tech.* **44** (suppl 2) 143–6

Takala P, Hänninen H, Montonen J, Mäkijärvi M, Nenonen J, Oikarinen L, Simelius K, Toivonen L and Katila T 1999 Comparison of Magnetocardiographic and electrocardiographic exercise mapping in healthy volunteers *Recent Advances in Biomagnetism: Proc. 11th Int. Conf. on Biomagnetism* (Sendai: Tohoku University Press) pp 306–9

Van Leeuwen P, Hailer B, Lange S, Donker D and Grönemeyer D 1999 Spatial and temporal changes during the QT-interval in the magnetic field of patients with coronary artery disease *Biomed. Tech.* **44** (suppl 2) 139–42